Molecular Cell, Vol. 12, 1427–1437, December, 2003, Copyright ©2003 by Cell Press

The Structure of the APPBP1-UBA3-NEDD8-ATP Complex Reveals the Basis for Selective Ubiquitin-like Protein Activation by an E1

Helen Walden,[1,4] Michael S. Podgorski,[1,4] Danny T. Huang,[1] David W. Miller,[1] Rebecca J. Howard,[2] Daniel L. Minor, Jr.,[2] James M. Holton,[3] and Brenda A. Schulman[1,*]

[1]Departments of Structural Biology and Genetics/Tumor Cell Biology
St. Jude Children's Research Hospital
Memphis, Tennessee 38105

[2]Cardiovascular Research Institute and Departments of Biochemistry and Biophysics and Cellular and Molecular Pharmacology
University of California, San Francisco
San Francisco, California 94143

[3]Lawrence Berkeley National Laboratory
1 Cyclotron Road
MS 6-2100
Berkeley, California 94720

Summary

E1 enzymes initiate ubiquitin-like protein (ubl) transfer cascades by catalyzing adenylation of the ubl's C terminus. An E1's selectivity for its cognate ubl is essential because the E1 subsequently coordinates the ubl with its correct downstream pathway. We report here the structure of the 120 kDa quaternary complex between human APPBP1-UBA3, a heterodimeric E1, its ubl NEDD8, and ATP. The E1 selectively recruits NEDD8 through a bipartite interface, involving a domain common to all ubl activating enzymes including bacterial ancestors, and also eukaryotic E1-specific sequences. By modeling ubiquitin into the NEDD8 binding site and performing mutational analysis, we identify a single conserved arginine in APPBP1-UBA3 that acts as a selectivity gate, preventing misactivation of ubiquitin by NEDD8's E1. NEDD8 residues that interact with E1 correspond to residues in ubiquitin important for binding the proteasome and other ubiquitin-interacting proteins, suggesting that the conjugation and recognition machineries have coevolved for each specific ubl.

Introduction

Posttranslational modification by ubiquitin and ubiquitin-like proteins (ubls) has emerged as an essential cellular regulatory mechanism. While the best-characterized consequence of these modifications is proteasome-dependent degradation of multiubiquitinated proteins (reviewed in Rechsteiner, 1998), other functions of ubiquitin and ubls also play fundamental regulatory roles. For example, multiubiquitin chains with linkages via Lys63, rather than the Lys48 linkages involved in proteasomal degradation, activate I_KB kinase (Deng et al., 2000), and monoubiquitylation plays a role in processes ranging from transcription to subcellular localization (reviewed in Hicke, 2001). The fate of the ubiquitinated protein is determined by interactions with downstream effector machineries such as the proteasome, which contain UBA (*ub*iquitin-*a*ssociated), UIM (*u*biquitin-*i*nteracting *m*otif), CUE (*c*oupling of *u*biquitin conjugation to *E*R degradation), or other domains that selectively recognize monoubiquitin or multiubiquitin chains with a particular linkage (Chen et al., 2001; Finley, 2002; Fisher et al., 2003; Kang et al., 2003; Lam et al., 2002; Polo et al., 2002; Prag et al., 2003; Shih et al., 2002, 2003; Wilkinson et al., 2001).

In addition to different ubiquitin modifications, many other ubl covalent modifiers alter the function of their important targets (Schwartz and Hochstrasser, 2003), and modification of a protein by different ubls leads to different biological consequences (Hoege et al., 2002). For example, SUMO family members are conjugated to proteins involved in cell division, the stress response, nuclear transport, and signal transduction (reviewed in Hay, 2001; Melchior, 2000; Muller et al., 2001); Apg12p and Apg8p/Aut7p/Cvt5p conjugates are required for autophagy (reviewed in Ohsumi, 2001); ISG15 is involved in the interferon response (Loeb and Haas, 1992); and Hub1p regulates cell polarity (Dittmar et al., 2002). The ubl NEDD8 (Rub1p in *S. cerevisiae*) modifies cullins and enhances SCF ubiquitin ligase activity (Lammer et al., 1998; Liakopoulos et al., 1998; Osaka et al., 1998) at least in part by displacing the CAND1 inhibitor (Liu et al., 2002; Zheng et al., 2002). As a result, the NEDD8 pathway is essential for cell division in organisms ranging from fission yeast to mammals (Osaka et al., 2000; Tateishi et al., 2001), and is also important for development (Pozo et al., 1998), cytokinesis (Kurz et al., 2002), and signal transduction (Amir et al., 2002; Read et al., 2000).

The diversity of fates awaiting a protein after modification by one or more ubls highlights the importance of coordinating the ubl with the correct target. Selectivity is dictated by a parallel but distinct cascade of enzymes for each ubl (reviewed in Hochstrasser, 2000). Many ubls including ubiquitin are synthesized as inert precursors that are cleaved to produce mature protein with a C-terminal Gly-Gly motif. Ubiquitin and many ubls are then conjugated via an isopeptide linkage between their C terminus and a primary amino group on the target by an enzymatic cascade that sequentially involves an E1 activating enzyme, an E2 conjugating enzyme, and an E3 ligase (reviewed in Pickart, 2001). First, the E1 activates the ubl's C terminus. In this step, the E1 binds the ubl, Mg^{2+}, and ATP and catalyzes adenylation of the ubl's C terminus. The E1 subsequently forms a thioester intermediate between its catalytic cysteine and the ubl C terminus, and then transfers the thioester-bound ubl to the E2's catalytic cysteine. The E3 recruits the target and facilitates ubl transfer from the E2 to the target.

E1s select the correct ubl for the pathway, in addition to their essential role in initiating ubl conjugation cascades (Finley et al., 1984; Hochstrasser, 2000). Each ubl has a dedicated E1, which exhibits remarkable specific-

*Correspondence: brenda.schulman@stjude.org
[4]These authors contributed equally to this work.

ity. For example, despite the fact that ubiquitin and NEDD8 are nearly 60% identical and have strikingly similar structures, they are distinguished by their own E1s. Ubiquitin's E1 only activates ubiquitin, and NEDD8's E1 only activates NEDD8 (Osaka et al., 1998; Whitby et al., 1998). This specificity is crucial because the E1 also transfers the ubl to its cognate E2, thereby coordinating the ubl with its correct downstream pathway. Therefore, an important question is how E1s specifically recognize only their particular ubl.

E1s exist as one of two 110–120 kDa forms: either a single polypeptide, such as the E1 for ubiquitin, or a heterodimeric complex, such as the E1 for NEDD8 (reviewed in Hochstrasser, 2000). In the heterodimeric E1s, one subunit (APPBP1 for NEDD8) corresponds to the N-terminal half of the single-chain E1s, and the other (UBA3 for NEDD8) corresponds to the C-terminal half. Both halves of E1 share a region of sequence homology with each other, and with the bacterial enzymes MoeB and ThiF, which catalyze a similar activation reaction as part of the molybdopterin and thiamin biosynthetic pathways, respectively. Like E1s, MoeB and ThiF catalyze adenylation of the C termini of MoaD and ThiS, structural homologs of ubiquitin and ubls that are parts of *E. coli* biosynthetic enzymes (Lake et al., 2001; Wang et al., 2001). Crystal structures have recently been determined for human APPBP1-UBA3, the E1 for NEDD8, and *E. coli* MoeB-MoaD complexes (Lake et al., 2001; Walden et al., 2003). The structures reveal that E1s have three domains: an evolutionarily conserved domain resembling *E. coli* MoeB, and two eukaryotic E1-specific domains. However, accurate docking of NEDD8 in the APPBP1-UBA3 structure was precluded by significant structural differences between NEDD8 and MoaD (3.0 Å rmsd over 65 residues) (Lake et al., 2001; Whitby et al., 1998), and occlusion of the NEDD8 binding site by an E1-specific domain. To address how an E1 recognizes its ubl in order to initiate the transfer cascade, we determined the crystal structure of the human APPBP1-UBA3-NEDD8 complex at 3.0 Å, and an additional APPBP1-UBA3-NEDD8 complex with ATP. These structures reveal how an E1 selects its particular ubl for activation.

Results and Discussion

Structure Determination of the APPBP1-UBA3-NEDD8 Complexes

In order to understand initial recognition of a ubl by its E1, and to obtain a pure complex for crystallization, all results reported here use a mutant version of APPBP1-UBA3, with UBA3's catalytic Cys216 mutated to alanine. In addition, we used a truncated version of NEDD8 terminating at Gly76, representing the active form. The structure of an APPBP1-UBA3-NEDD8 complex lacking a loop from APPBP1 (residues 254–258) and the N-terminal 11 residues of UBA3 was refined at 3.0 Å, with four copies in the asymmetric unit (Table 1; Figure 1) (Experimental Procedures). A subset of the noncrystallographic symmetry (NCS) packing interactions are similar to those found in the apo APPBP1-UBA3 crystals (Walden et al., 2003), so we measured the molecular weight of APPBP1-UBA3 by analytical ultracentrifugation. The measured molecular weight of 106.6 kDa is consistent with the value of 110.1 kDa calculated for the APPBP1-UBA3 heterodimer (data not shown). All four copies of APPBP1-UBA3-NEDD8 in the asymmetric unit are essentially identical (rmsds ranging from 0.08 to 0.1 Å), so discussion focuses on only one. To gain additional insights into the activation reaction, we soaked the APPBP1-UBA3-NEDD8 crystals in ATP to obtain a second structure containing ATP, refined at 3.6 Å.

Table 1. Data and Refinement Statistics

	APPBP1-UBA3-NEDD8	APPBP1-UBA3-NEDD8-ATP
Resolution (Å)	3.0	3.6
No. observations	2,787,084	2,710,454
No. unique observations	113,171	66,111
Completeness (%)	100 (99.9)	97.9 (94.4)
R_{merge}[a] (%)	10.9 (59.6)	8.7 (36.1)
$I/\sigma I$	17.1 (1.8)	12.6 (1.9)
Mean redundancy	24.6	41
Refinement statistics		
Protein/Zn/ATP atoms	31,628/4/0	31,628/4/124
$R(R_{free})$[a] (%)	24.0 (28.0)	25.1 (29.0)
Rmsd bond length (Å)	0.008	0.01
Rmsd bond angles (°)	1.35	1.45

[a] $R_{merge} = \Sigma|I(k) - [I]|/\Sigma I(k)$, where $I(k)$ is the value of the kth measurement of the intensity of a reflection, $[I]$ is the mean value of the intensity of that reflection, and the summation is of all the measurements. Brackets denote the last resolution shell, 3.1–3.0 Å in the APPBP1-UBA3-NEDD8 experiment, 3.7–3.6 Å in the ATP experiment. $R = \Sigma|F_{obs} - F_{calc}|/\Sigma|F_{obs}|$, where F_{obs} and F_{calc} are the observed and calculated structure factors, respectively, with a cutoff criterion of $|F| > 0\sigma$. R_{free} = R calculated with 5% of the reflection data chosen randomly and omitted from the start of refinement.

Overall Structure of the APPBP1-UBA3-NEDD8-ATP Complex

Structures of NEDD8 and APPBP1-UBA3 alone have been described previously. The structure of NEDD8 (Whitby et al., 1998), like ubiquitin and other ubls (Bayer et al., 1998; Vijay-Kumar et al., 1985) has two regions: a globular body comprising a five-stranded mixed β sheet and an α helix, and a flexible C-terminal tail with the Gly-Gly motif at the C terminus. NEDD8 and ubiquitin both have an asymmetric distribution of charged residues. One face of NEDD8 is predominantly acidic. The opposite face contains the Leu8/Ile44/Val70 hydrophobic patch (Beal et al., 1996; Whitby et al., 1998).

The E1, APPBP1-UBA3, is a multidomain heterodimer, with an adenylation domain conserved in ubl activating enzymes throughout evolution linked through flexible loops to two eukaryotic E1-specific domains (Walden et al., 2003). The adenylation domain portion of UBA3, which is structurally homologous to *E. coli* MoeB (Lake et al., 2001; Walden et al., 2003), contains the Gly-X-Gly-X-X-Gly ATP binding motif (Walker et al., 1982). One of the E1-specific domains contains UBA3's catalytic cysteine involved in the thioester intermediate, and the other domain, at the C terminus, is involved in ubl transfer to E2. The overall APPBP1-UBA3 structure resembles a canyon, with a large groove in the middle. An 8 residue "crossover loop" (VanDemark and Hill, 2003) leads from the adenylation domain to the catalytic cys-

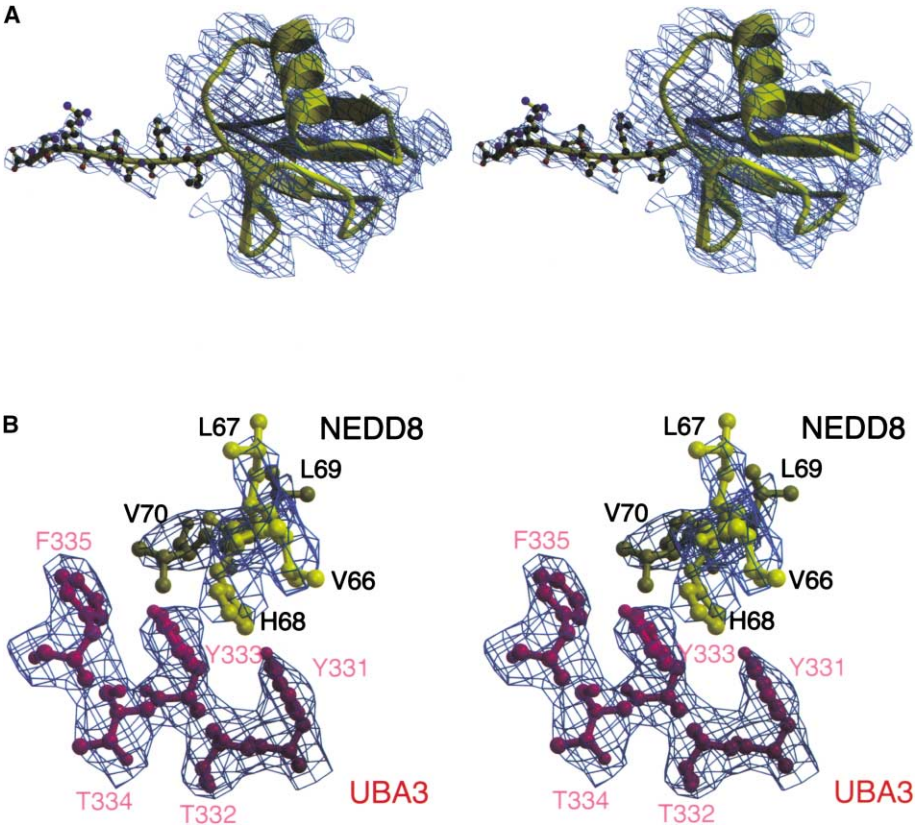

Figure 1. Stereo Views of Electron Density Maps

(A) NEDD8 displayed in the initial NCS-averaged 2Fo-Fc map contoured at 1.5σ, calculated from the original model lacking NEDD8.
(B) Detail from the final refined 2Fo-Fc map showing NEDD8 interaction with UBA3 contoured at 1.5σ.

teine, and divides the canyon into two clefts. The two clefts are continuous with each other below and above the crossover loop. The large size of the two clefts in the apo APPBP1-UBA3 structure suggested that the clefts function to accommodate the E1's protein substrates (Walden et al., 2003).

In the quaternary complex, NEDD8 fits snugly in the groove in the middle of APPBP1-UBA3, in a manner resembling a baseball in a mitt (Figure 2). NEDD8's globular domain fits in one cleft in the APPBP1-UBA3 structure. The C-terminal tail extends under the crossover loop into the other cleft, toward ATP. NEDD8's C terminus is located within 4 Å of ATP's α-phosphate, poised for the adenylation reaction.

APPBP1-UBA3 binds NEDD8 through a bipartite interface, involving both the conserved adenylation domain and the E1-specific catalytic cysteine-containing domain. From NEDD8, both the acidic and hydrophobic surfaces of the globular domain, as well as the C-terminal tail contact E1, resulting in an extensive protein-protein interaction burying ~3350 Å^2 and 34% of NEDD8 (Figures 2 and 3). NEDD8's acidic face contacts a charged surface on the E1-specific catalytic cysteine domain portion of APPBP1. The opposite, hydrophobic face of NEDD8 contacts a hydrophobic surface on the adenylation domain portion of UBA3. NEDD8's C-terminal tail, continuous with the hydrophobic surface, extends away from the globular domain in a rigid manner. The C-terminal tail sits in a very shallow channel on the surface of UBA3 and is clamped against UBA3 by the crossover loop. At the end of the tail, NEDD8's C terminus is inserted into the deeper ATP binding pocket in UBA3.

NEDD8 Recognition by APPBP1-UBA3: Implications for Ubl-E1 Interactions

We describe the details of the interface between NEDD8 and APPBP1-UBA3 in three portions: (1) the polar interface between the acidic face of NEDD8 and an E1-specific domain of APPBP1, (2) the hydrophobic interface between the opposite face of NEDD8 and the conserved adenylation domain of UBA3, and (3) the interactions between NEDD8's C-terminal tail and UBA3's adenylation domain and crossover loop.

The acidic face of NEDD8's globular domain interacts extensively with the catalytic cysteine domain portion of APPBP1 (Figures 3 and 4A). This interface involves the helix and subsequent loop in NEDD8 and a subdomain comprising APPBP1's residues 178–280 that serves as a wall for the broad, deep groove in the APPBP1-UBA3 structure. This portion of the interface is unique to eukaryotic E1s and is not found in distal bacterial relatives such as MoeB (Lake et al., 2001). The nature of this interface is predominantly polar, with 11 residues from NEDD8 forming a network of hydrogen bonds and salt bridges with 9 residues from APPBP1, burying

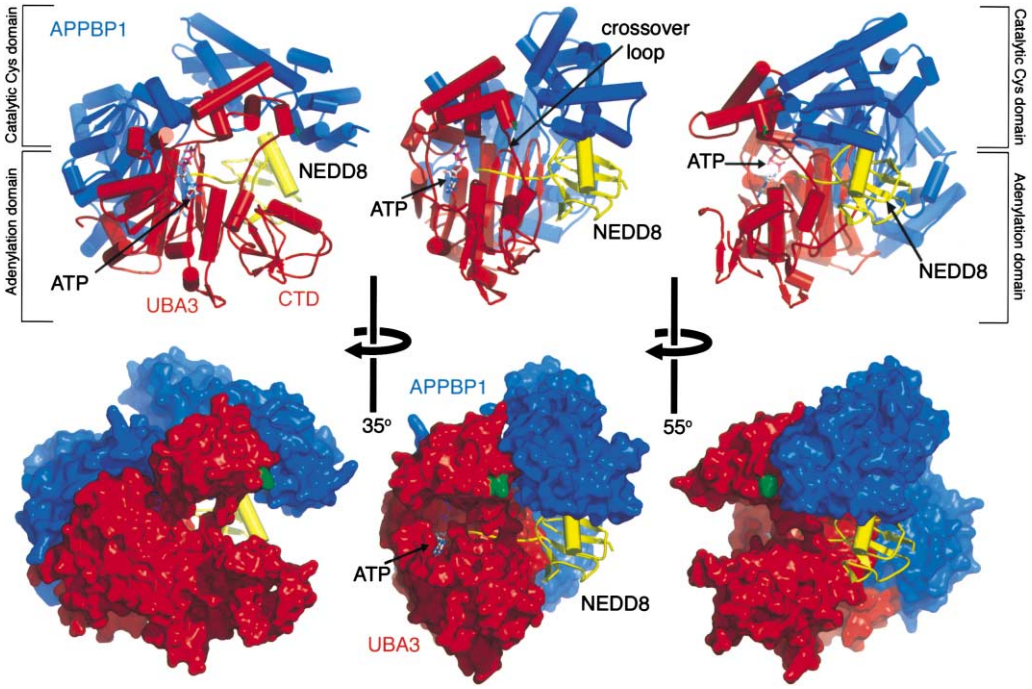

Figure 2. Overall Structure of the APPBP1-UBA3-NEDD8-ATP Complex

Three views of the complex are shown in cartoon (top) and space-filling representations (bottom), each view a 35°–55° rotation around the *y* axis as indicated. APPBP1 is shown in blue, UBA3 in red, NEDD8 in yellow, and the position of the catalytic cysteine (C216A here) in green. The location of ATP is indicated in each view in the cartoon representations. The adenylation domain, the catalytic cysteine domain, and the C-terminal domain (CTD) are indicated. Figures were made using Pymol (DeLano, 2002).

~810 Å^2 surface area. Comparison of the sequences of NEDD8 and ubiquitin reveals a high degree of conservation in E1-interacting residues from this polar interface. NEDD8's Gly35, Ile36, Lys33, Pro37, and Gln40 are identical in ubiquitin, and there are conservative substitutions at Arg25, Arg29, Glu31, Glu32, and Glu34, suggesting that these residues in ubiquitin will be involved in similar polar interactions with the catalytic cysteine domain of ubiquitin's E1.

The hydrophobic patch on the opposite face of the globular domain of NEDD8 contacts UBA3's adenylation domain, which is structurally conserved in activating enzymes throughout evolution (Lake et al., 2001; Walden et al., 2003). Here, NEDD8 interacts with the four-

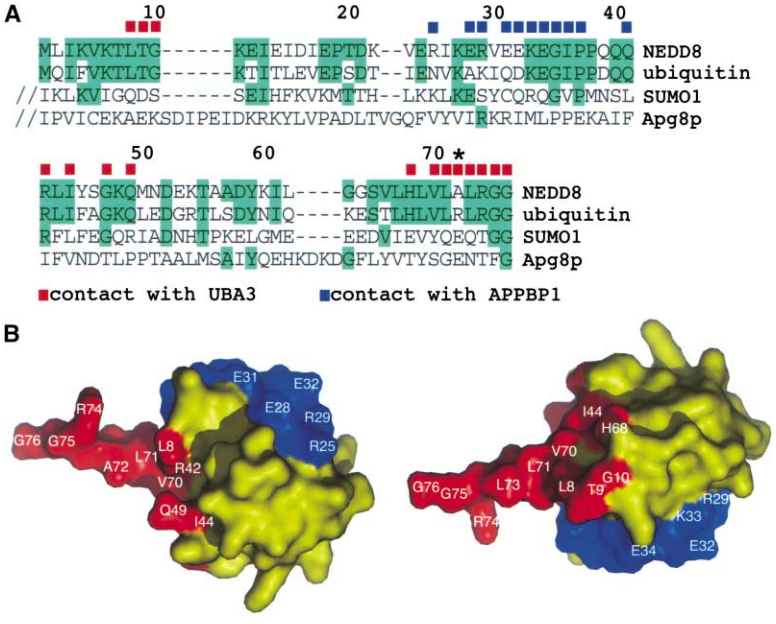

Figure 3. NEDD8's E1-Interacting Surfaces

(A) Sequence alignment of human NEDD8, ubiquitin, and SUMO1 and *S. cerevisiae* Apg8p. Residues identical to NEDD8 are shaded. The asterisk above the sequence alignment denotes a known specificity determinant in ubls. (B) Two views of NEDD8 rotated 180° in x. Residues contacting UBA3 are shown in red, and those contacting APPBP1 in blue.

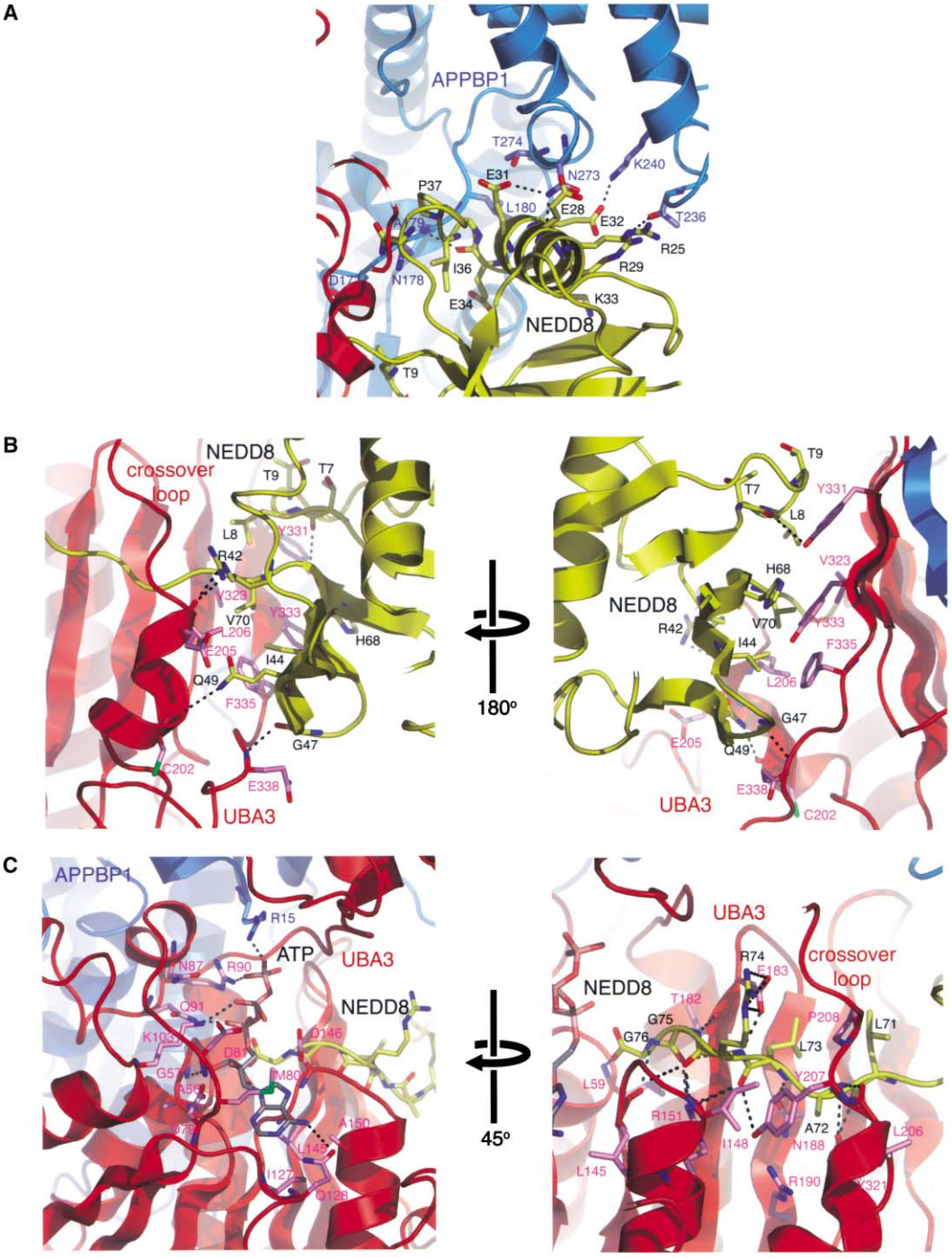

Figure 4. Detailed Views of NEDD8 and ATP Interactions with APPBP1-UBA3

APPBP1 is shown in blue, UBA3 in red, and NEDD8 in yellow. Nitrogen atoms are highlighted in blue, oxygen atoms in red. Hydrogen bonds are dashed.

(A) Close-up view of interactions between the E1's catalytic cysteine domain and NEDD8's polar surface.

(B) Interface between hydrophobic surfaces in NEDD8 and UBA3 shown in two views rotated 180° in *y*. The left view is in an orientation similar to the middle view in Figure 2.

(C) Interactions between NEDD8's C-terminal tail and ATP with the adenylation domain and crossover loop of UBA3 shown in two views, rotated 45° in *y*. For ATP, carbon atoms are shown in gray, and phosphates in peach. The left panel is in a similar orientation to the left view in Figure 2. The right panel is in a similar orientation to the middle view in Figure 2.

stranded β sheet preceding UBA3's C-terminal domain, and the NEDD8-interacting residues in this region are exclusively from UBA3, with no involvement of APPBP1. This interaction is predominantly hydrophobic, centered around NEDD8's Leu8/Ile44/Val70 hydrophobic patch interacting with UBA3's Val323, Tyr331, Tyr333, and

Phe335, and there is also ring-stacking between NEDD8's His68 and UBA3's Tyr333 (Figures 3 and 4B). The importance of NEDD8 interacting with this region of UBA3 is underscored by the previous finding that mutation of UBA3's Tyr331, Tyr333, and Phe335 reduced the ability of APPBP1-UBA3 to promote NEDD8-adenylate formation (Walden et al., 2003). In addition to hydrophobic contacts, this interaction is stabilized by hydrogen bonds and salt bridges between 4 residues in each NEDD8 and UBA3, including between NEDD8's Arg42 and the carbonyl of UBA3's Glu205. All of NEDD8's key residues involved in this interaction are identical in ubiquitin, and several of them play a critical role in ubiquitin conjugation. Ubiquitin's Leu8, Arg42, Ile44, and Val70 are essential for yeast viability (Sloper-Mould et al., 2001), and mutation of ubiquitin's Leu8, or Leu8 in combination with Val70, reduces ubiquitin-conjugate formation (Beal et al., 1996). In addition, mutation of ubiquitin's Arg42 to leucine reduces the E1's affinity for ubiquitin-adenylate by three orders of magnitude (Burch and Haas, 1994).

NEDD8's C-terminal tail extends away from the hydrophobic patch, and sits in a shallow groove in the adenylation domain portion of UBA3, under the crossover loop (Figures 2 and 4C). $\sim$2530 Å^2 surface area is buried upon NEDD8's C-terminal tail and hydrophobic patch binding to UBA3. At the beginning of the tail, NEDD8's Leu71 and Ala72 interact with UBA3's Leu206, Tyr207, and Pro208 in the crossover loop. The importance of these interactions is highlighted by the previous finding that mutation of UBA3's Leu206 and Tyr207 in the crossover loop reduces the ability of APPBP1-UBA3 to promote adenylation of NEDD8 (Walden et al., 2003). The four remaining C-terminal residues in NEDD8 make extensive contacts with ten residues from UBA3's adenylation domain. Every residue in NEDD8's C-terminal tail is identical in ubiquitin except the specificity determining residue, Ala72, and ubiquitin's C-terminal tail residues are all essential for yeast viability (Sloper-Mould et al., 2001). In addition, ubiquitin's Arg74 and Gly76 have been shown to play critical roles in ubiquitin activation: mutation of Arg74 to leucine reduces the catalysis of ATP:PPi exchange (Burch and Haas, 1994), and mutation of Gly76 to alanine greatly decreases ubiquitin-adenylate formation (Pickart et al., 1994).

The striking conservation of E1-interacting residues between NEDD8 and ubiquitin strongly suggests that ubiquitin interacts with its E1 in a manner resembling NEDD8's interaction with APPBP1-UBA3. It is likely that other ubls interact with their E1s in a similar manner.

The ATP Binding Site

ATP binds adjacent to NEDD8's C terminus in a pocket centered around UBA3's Gly-X-Gly-X-X-Gly nucleotide binding motif (Walker et al., 1982) (Figure 4C). The nucleotide binding pocket forms a T shape with the shallow channel holding NEDD8's C-terminal tail. ATP's α-phosphate and NEDD8's C terminus form the junction of the T.

ATP's adenine ring interacts with a hydrophobic patch in UBA3, involving Met80, Ile127, Leu145, and Ala150. Leu145 and Ala150 are identical in the E1s for ubiquitin and SUMO, and these residues are all hydrophobic in other activating enzymes. The N7 position of ATP forms a hydrogen bond with UBA3's Asp146, which is identical in all ubl activating enzymes, and the N1 amino group forms a hydrogen bond with Gln128. The ribose ring contacts Ala56 and Gly57 of the nucleotide binding motif, and Asp79 and Asp81. ATP's α-phosphate forms salt bridges with UBA3's Arg90 and Lys103 and a hydrogen bond with Gln91, its β-phosphate forms a hydrogen bond with Asn87, and its γ-phosphate forms salt bridges with UBA3's Arg90 and APPBP1's Arg15. Every side chain that contacts ATP's phosphates is identical among ubl activating enzymes. Although Mg^{2+} is not present in either structure, the side chain of UBA3's Asp146 is in a position to coordinate the Mg^{2+} ion. The importance of ATP binding in this region is reflected by the previous finding that mutating residues in the ATP binding site impairs NEDD8 adenylation (Walden et al., 2003).

The structure is consistent with the mechanism for ubl activation proposed previously based on the *E. coli* MoeB-MoaD structure (Lake et al., 2001). For NEDD8, this would involve Mg^{2+} coordinated by Asp146 interacting with ATP's β- and γ-phosphates, NEDD8's C terminus attacking the ATP's α-phosphate to generate a pentacoordinated intermediate, and UBA3's Arg90 and Lys103 and APPBP1's Arg15 stabilizing the developing negative charge to facilitate formation of NEDD8-adenylate and inorganic pyrophosphate. The strong conservation in the ATP binding site is consistent with the notion that the catalytic mechanism of ubl activation is conserved throughout evolution.

Evolution of an E1 from an Ancestral Ubl Activating Enzyme

E1s are thought to have evolved from the bacterial enzymes MoeB and ThiF, which catalyze a similar adenylation reaction as part of biosynthetic pathways (reviewed in Hochstrasser, 2000). Indeed, the structures of the ATP binding regions of APPBP1-UBA3 and MoeB are very similar (Lake et al., 2001; Walden et al., 2003). The APPBP1-UBA3-NEDD8 structure reveals that, despite low sequence homology, part of the E1's ubl binding site resembles *E. coli* MoeB's binding site for MoaD. The APPBP1-UBA3-NEDD8 structure also reveals how E1-specific structures have evolved to carry out E1-specific functions, such as E1-ubl thioester formation and ubl transfer to E2, while eliminating unwanted ancestral functions. For example, E1s like APPBP1-UBA3 activate only one ubl molecule at a time in preparation for downstream reactions in the pathway (Haas et al., 1982), unlike MoeB, which is a symmetric homodimer that simultaneously activates two molecules of MoaD (Lake et al., 2001). E1s restrict ubl binding to the half of the MoeB-homology region that faces the catalytic cysteine, to drive the next step of the reaction cascade. The E1 evolved a second part to the ubl interaction surface, from the E1-specific catalytic cysteine-containing domain, to recruit NEDD8 to a single binding site for activation. The finding that the catalytic cysteine domain helps recruit NEDD8 for adenylation indicates that the different domains in the E1 structure are multifunctional. Rather than serving as distinct modules with their own individual functions, the different domains in

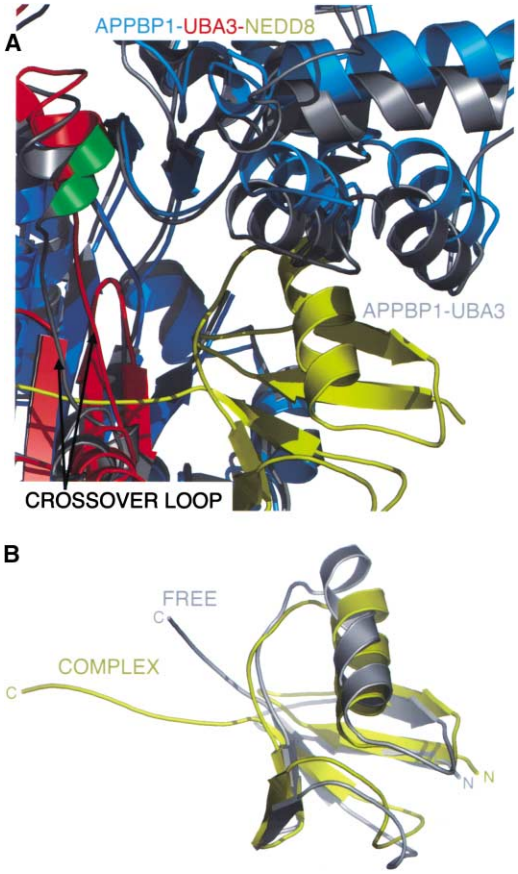

Figure 5. Conformational Changes in APPBP1-UBA3 and NEDD8 Accompanying Complex Formation

(A) Superposition of the APPBP1-UBA3-NEDD8 complex structure (blue-red-yellow) with the previous apo APPBP1-UBA3 structure (gray). The catalytic cysteine domain and crossover loop undergo conformational changes.

(B) Superposition of free (gray) (Whitby et al., 1998) and APPBP1-UBA3-bound (yellow) NEDD8 structures. The N and C termini are indicated. Superposition was performed by least-squares fitting over all Cα atoms.

the E1 structure work together to drive the initial steps of ubl transfer cascades.

Conformational Changes in APPBP1-UBA3 and NEDD8 upon Complex Formation: Implications for the E1 Reaction Cycle

Comparison of the APPBP1-UBA3-NEDD8 complex with the structures of free APPBP1-UBA3 (Walden et al., 2003) and NEDD8 (Whitby et al., 1998) reveals that both E1 and NEDD8 undergo significant conformational changes in order to drive the activation reaction (Figure 5). A conformational change in the E1 is required because the catalytic cysteine domain occludes the NEDD8 binding site in the apo APPBP1-UBA3 structure. A subdomain of the catalyic cysteine domain, comprising APPBP1's residues 178–280, moves away from the adenylation domain, widening the groove in the middle of the E1 to make room for NEDD8 (Figure 5A). This results from a ~10° rotation in hinges in two loops, about residues 180 and 280. In addition, UBA3's crossover loop moves ~2.5 Å to fasten NEDD8's C-terminal tail onto the adenylation domain. UBA3's Leu206, Tyr207, and Pro208 in the crossover loop serve as a clamp around NEDD8's Ala72 to secure NEDD8's C terminus in the active site.

The most striking difference between free (Whitby et al., 1998) and complexed NEDD8 is the C-terminal tail (Figure 5B), which rotates 30° about Leu69 to form the complex. Complex formation induces order in the C-terminal 3 residues, which are disordered in free NEDD8. The C-terminal tail adopts an extended β-strand-like conformation as it docks into the nucleotide binding pocket in UBA3.

These conformational differences between free and complexed APPBP1-UBA3 and NEDD8 reveal inherent flexibility in the loops linking the domains in the E1 and structural plasticity in NEDD8's C-terminal tail, raising the possibility of other comparable conformational changes driving downstream reactions in the transfer cascade. After ubl activation, the next step in the reaction cascade involves the E1's catalytic cysteine attacking the ubl-adenylate to form a thioester intermediate (reviewed in Pickart, 2001). Formation of the thioester between APPBP1-UBA3 and NEDD8 requires the active site cysteine, UBA3's Cys216, to contact NEDD8's C terminus. In the structure reported here, there is a ~35 Å gap between UBA3's residue 216 (here an alanine) and the C terminus of NEDD8 (Figure 2). The gap would be reduced by NEDD8's C-terminal tail pointing toward the catalytic cysteine, at an angle similar to that found in the structure of free NEDD8 (Whitby et al., 1998). The remaining gap can be closed by a rotation in the orientations of the E1's adenylation and catalytic cysteine domains, of a magnitude similar to the 10° rotation observed here, or by local conformational changes in the crossover loop and around the catalytic cysteine.

A Single Conserved Arginine in APPBP1-UBA3 Selects against Ubiquitin Activation

Each ubl has a dedicated E1, which catalyzes adenylation only of its cognate ubl. A major question in the ubiquitin and ubl-transfer pathways is how E1s select their particular ubl. The present structure reveals that APPBP1-UBA3 recognizes NEDD8 through an extensive interface. Many NEDD8 residues involved in the interaction are conserved in ubiquitin (Figure 3A), raising the question of why APPBP1-UBA3 activates NEDD8 but not ubiquitin. The only side chain that differs between ubiquitin and NEDD8 in the C-terminal tail is residue 72, which is arginine in ubiquitin, and alanine in NEDD8. Previous studies indicate that residue 72 is a key determinant for E1 recognition: mutation of NEDD8's Ala72 to arginine allows NEDD8 to be activated by ubiquitin's E1 (Whitby et al., 1998); and mutation of ubiquitin's basic Arg72 to leucine allows ubiquitin to be recognized by NEDD8's E1 (Bohnsack and Haas, 2003). Indeed, we find that mutation of NEDD8's Ala72 to arginine prevents APPBP1-UBA3 from promoting adenylation of NEDD8, and mutation of ubiquitin's Arg72 to alanine allows adenylation of ubiquitin (Figure 6).

An E1's selectivity is derived from differences in its affinities for different ubls. Both attractive and repulsive forces play a role in determining specificity. In the

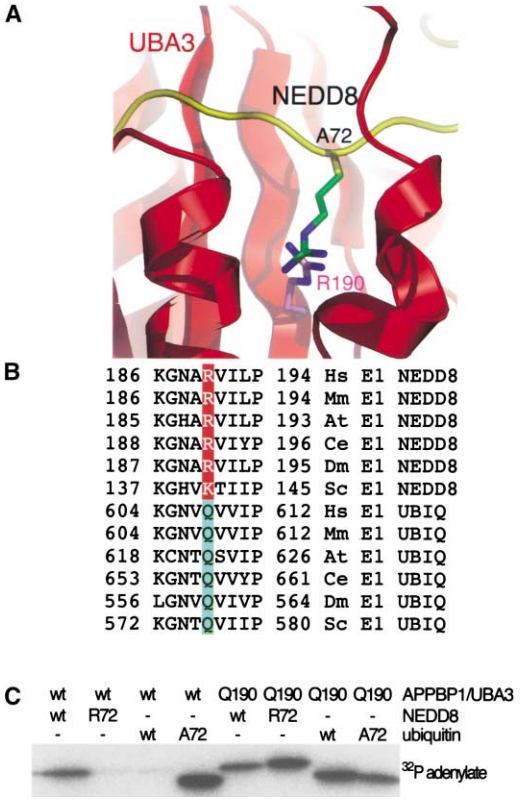

Figure 6. A Single Conserved Arginine in APPBP1-UBA3 Selects against Ubiquitin Activation

(A) Ubiquitin's Arg72 modeled into the position of NEDD8's Ala72. UBA3's Arg190 is shown clashing with the model.

(B) Sequence alignment showing absolute conservation of UBA3's Arg190 as a basic residue, and the E1 for ubiquitin's corresponding glutamine in the following organisms: Hs, human; Mm, *M. musculus*; At, *A. thaliana*; Ce, *C. elegans*; Dm, *D. melanogaster*; Sc, *S. cerevisiae*.

(C) In vitro adenylation assay with wild-type and mutant versions of APPBP1-UBA3, NEDD8, and ubiquitin. The UBA3 R190Q mutant is indicated as "Q190," the NEDD8 A72R mutant as "R72," and the ubiquitin R72A mutant as "A72." The transfer of [^{32}P]AMP from [α-^{32}P]ATP to the C terminus of either NEDD8 or ubiquitin is monitored as described in Experimental Procedures. ^{32}P-labeled NEDD8-adenylate and ubiquitin-adenylate are separated by SDS-PAGE, and detected by autoradiography. Differences in electrophoretic mobility between NEDD8-adenylate and ubiquitin-adenylate arise from an additional three residues on NEDD8 from cloning.

APPBP1-UBA3-NEDD8 structure, NEDD8's hydrophobic Ala72 interacts with UBA3's hydrophobic Leu206 and Tyr207 in the crossover loop. These favorable interactions may be preserved between other ubls and the crossover loops of their E1s, as the properties of residue 72 in other ubls corresponds with the properties of residues paralleling Leu206 and Tyr207 in other activating enzymes. The amino acids corresponding to NEDD8's Ala72 are an arginine in ubiquitin and a glutamate in SUMO-1 and Apg8p (Figure 3A), which could interact favorably with the aspartate, lysine, and arginine residues in the crossover loop sequences of the E1s for ubiquitin, SUMO, and Apg8p, respectively (Hatfield et al., 1990; Johnson et al., 1997; McGrath et al., 1991; Mizushima et al., 1998). However, while replacement of UBA3's Leu206 and Tyr207 with the corresponding aspartate in ubiquitin's E1 sequence diminishes NEDD8 activation, it is not sufficient to allow APPBP1-UBA3 to activate ubiquitin (Walden et al., 2003), raising the question of the identity of the E1's selectivity determinant.

In order to understand how an E1 selects against activating the wrong ubl, we modeled an arginine side chain into NEDD8's Ala72 position in the APPBP1-UBA3-NEDD8 structure (Figure 6A). The model suggests APPBP1-UBA3 cannot tolerate an arginine at NEDD8's position 72 because of repulsion from UBA3's Arg190. Consistent with this notion, UBA3's Arg190 is absolutely conserved as a basic residue from yeast to mammals (Figure 6B). By contrast, the corresponding residue in ubiquitin's own E1 is an absolutely conserved glutamine, which could promote interaction with an arginine side chain, rather than repelling it. We tested the role of UBA3's Arg190 in selecting against an arginine at NEDD8's or ubiquitin's position 72: mutation of UBA3's Arg190 to glutamine allows adenylation of both the NEDD8 A72R mutant and ubiquitin (Figure 6C). These results demonstrate that a single conserved arginine in APPBP1-UBA3 acts as a selectivity gate, preventing the misactivation of ubiquitin by NEDD8's E1.

Selectivity of Ubiquitin and Ubl Pathways

The APPBP1-UBA3-NEDD8 structure reveals that the NEDD8 conjugation machinery interacts with a multipurpose binding site on the ubl. NEDD8's Leu8/Ile44/Val70 hydrophobic patch involved in the interaction with APPBP1-UBA3 is absolutely conserved in ubiquitin. In ubiquitin, this hydrophobic patch was originally identified as the site of proteasome binding (Beal et al., 1996). More recently, ubiquitin's hydrophobic patch has been shown to be involved in interactions with UBA, UIM, and CUE domains found in ubiquitin recognition machineries involved in endocytosis, ER protein sorting, vacuolar protein sorting, and other functions (Chen et al., 2001; Fisher et al., 2003; Kang et al., 2003; Polo et al., 2002; Prag et al., 2003; Shih et al., 2002, 2003; Wilkinson et al., 2001). The finding that an E1 and these ubiquitin recognition domains all interact with a common surface suggests that ubl conjugation and effector machineries have coevolved to distinguish their cognate ubl.

Just as ubl conjugation machinery has evolved specificity to ensure that the correct modification is coordinated with the correct target, the ubl recognition machinery must also distinguish between modifications. For example, the proteasome recognizes multiubiquitin chains linked between Lys48 on the surface of one ubiquitin and the C terminus of the next. On the other hand, some UBA, UIM, and CUE domains interact with monoubiquitin. It is likely that the functions of other ubl modifications will be executed through their interaction with selective recognition machineries. The APPBP1-UBA3-NEDD8 structure reveals two mechanisms for establishing specificity. Comparison of the APPBP1-UBA3-NEDD8 and MoeB-MoaD structures (Lake et al., 2001) suggests that global differences in ubl sequences and structures likely account for much specificity. The APPBP1-UBA3-NEDD8 structure also reveals how very closely related ubls can be distinguished. We find that

a single residue in the 110 kDa E1 acts as a barrier that prevents misactivation of ubiquitin by NEDD8's E1. Thus, in addition to recognition *for* NEDD8, discrimination *against* ubiquitin plays a major role in the E1's selectivity. Selection against interactions with incorrect ubls may prove to be a common mechanism for establishing specificity of ubl pathways.

Experimental Procedures

Protein Expression and Purification

All variants of human APPBP1-UBA3 used for crystallization trials were purified as described previously (Walden et al., 2003). NEDD8 used for crystallization was expressed as a GST-fusion from pGEX4T1 (Amersham Biosciences) with a GGS linker inserted to facilitate thrombin cleavage. GST-NEDD8 was purified by glutathione affinity and anion exchange chromatography prior to thrombin cleavage and gel filtration. APPBP1-UBA3 variants were mixed overnight with a 2-fold excess of NEDD8 in 50 mM Tris, 150 mM NaCl, 5 mM $MgCl_2$, 5 mM ATP, and 5 mM DTT (pH 7.6). The ternary complex was isolated from unbound NEDD8 by gel filtration and concentrated to 15–30 mg/ml. Although ATP and Mg^{2+} were present during ternary complex formation, mass spectrometry and, subsequently, electron density maps revealed no indication of covalent modification of NEDD8's C terminus. Hydrolysis of ubiquitin-adenylate has been observed previously during gel filtration chromatography (Haas et al., 1982). The use of protein concentrations 250-fold greater than the Km (Bohnsack and Haas, 2003) likely stabilized the ternary complex. In vitro adenylation assays use GST-APPBP1-UBA3 C216A complexes purified as described previously (Walden et al., 2003), and use NEDD8 and ubiquitin expressed as GST-fusions from pGEX2TK, purified by glutathione affinity chromatography prior to thrombin cleavage, and further purified by gel filtration. The resulting NEDD8 has three more residues than ubiquitin upstream of the N-terminal methionine due to differences in cloning. Mutations were introduced by PCR. The entire coding sequence for each construct was verified by sequencing.

Crystallization, Data Collection, Structure Determination, and Refinement

We were unable to obtain high-quality crystals of full-length APPBP1-UBA3-NEDD8. Thus, we tested deletions lacking sequences disordered in previous apo APPBP1-UBA3 crystals (Walden et al., 2003). Mutants lacking UBA3's N-terminal 11 or C-terminal 92 residues formed soluble complexes; further deletions led to aggregation. Although complexes with C-terminal deletions failed to crystallize, we obtained irreproducible crystals of poor quality of a complex lacking UBA3's residues 1–11. Crystals of APPBP1-UBA3-NEDD8 complexes from different constructs were grown by the hanging-drop vapor diffusion method in 10.5%–10.7% PEG 10k, 0.1 M Tris, 0.4 M NaCl, 10% PEG400, 5 mM DTT (pH 8.0–8.5) at 18°C. The crystals form in $P2_12_12_1$, with a = 135.4 Å, b = 198.9 Å, c = 209.8 Å, with four complexes in the asymmetric unit. Crystals were flash-frozen in 13% PEG 10k, 50 mM Tris, 0.2 M NaCl, 5% PEG400, 5 mM DTT, 30% ethylene glycol (pH 8.0–8.5), prior to data collection. We obtained one diffraction quality crystal of this complex, and collected data to 3.6 Å at SERCAT at the Advanced Photon Source (APS). The structure was determined by molecular replacement using the program AMORE (Navaza, 1994). We did not determine the structure using the apo APPBP1-UBA3 as a search model, likely due to conformational changes accompanying complex formation. In the process of identifying a suitable molecular replacement model, we noticed an approximate doubling of one cell edge relative to apo APPBP1-UBA3 crystals (Walden et al., 2003). Thus, we anticipated similar NCS packing in the NEDD8-bound complex. The two copies of the adenylation domain in the asymmetric unit of apo APPBP1-UBA3 (APPBP1 residues 9–168 and 486–534; UBA3 residues 19–240 and 290–347) were used as a search model. Two solutions were found with a correlation coefficient of 0.54 and R factor of 0.47, indicating four complexes in the asymmetric unit. The remaining portions of APPBP1 and UBA3 were well defined in a 2Fo-Fc map calculated from the initial solution. After building the APPBP1-UBA3 structure, the entire sequence of NEDD8 was located in an NCS averaged map (Figure 1). Examination of crystal contacts revealed a loop in APPBP1 (residues 254 and 258) located next to a symmetry mate, potentially restricting crystal quality. Crystal reproducibility and diffraction quality improved considerably upon removal of this loop, allowing collection of data to 3.0 Å at the 8.3.1 beamline at the Advanced Light Source (ALS). The original model was refined using CNS (Brünger et al., 1998) against the 3.0 Å data set, with a final R factor of 24.0% and R_{free} of 28.0% (Table 1). The final model contains NEDD8 residues 1–76; APPBP1 residues 6–199, 209–253, and 259–534; and UBA3 residues 12–396 with 37 additional residues built as polyalanine owing to weak electron density for side chains in the C-terminal domain. Residues 200–208 of APPBP1 and 389 of UBA3 are not visible in the electron density maps and are presumably disordered.

The improvement in crystal quality upon loop removal allowed us to obtain an additional ATP-bound structure. Crystals of the APPBP1-UBA3-NEDD8 complex lacking APPBP1's 254–258 loop and UBA3's N-terminal 11 residues were soaked for 18 hr in 13% PEG 10k, 0.1M Tris-Cl, 0.4 M NaCl, 5 mM DTT, and 20 mM ATP, pH 8.0 prior to flash freezing and data collection at the SERCAT beamline at APS. The model was refined against these data, and clear density for ATP was visible in an Fo-Fc map plotted at 3σ for all four copies of the complex in the asymmetric unit. This model was refined to 3.6 Å, with a final R factor of 25.1% and R_{free} of 29.0% (Table 1). All data were processed using DENZO/SCALEPACK (Otwinowski and Minor, 1997).

Analytical Ultracentrifugation

Measurements were performed using a Beckman XL-A centrifuge equipped with an An-60 Ti rotor. Protein solutions were loaded at initial concentrations of 5, 20, and 100 μM in 10 mM Tris (pH 7.6), 150 mM NaCl, 0.5 mM DTT, and analyzed at rotor speeds of 6.5 and 8 krpm at 4°C. Data were acquired at 1–4 wavelengths for each concentration per rotor speed, and processed by nonlinear least-squares fitting.

In Vitro Adenylation Assays

NEDD8- and ubiquitin-adenylate formation was monitored by following attachment of ^{32}P AMP to NEDD8. 60 nM GST-APPBP1-UBA3 or mutant complex, 4.4 μM NEDD8 or ubiquitin, and 2 μCi [α-^{32}P]ATP were incubated for 2 min in 6 μl 25 mM Tris, 25 mM NaCl, 10 mM $MgCl_2$, and 0.4 mg/ml BSA (pH 7.6). Reactions were terminated with SDS-PAGE sample buffer. The NEDD8-^{32}P adenylate and ubiquitin-^{32}Padenylate were resolved from free ^{32}P-labeled ATP by SDS-PAGE.

Acknowledgments

We thank Steve Blacklow, Chris Garcia, Song Tan, Peter Murray, and Art Haas for helpful discussions. We thank Jon Huibregtse for the pGEX2TK-ubiquitin construct, and Charles Ross and the staff at the SERCAT beamline at APS and the staff at ALS synchrotron facilities for assistance. This work was supported by ALSAC, the NIH (P30CA21765 core grant to St. Jude, R01GM69530 to B.A.S.), and the Pew Scholars Program.

Received: September 9, 2003
Revised: October 10, 2003
Accepted: October 14, 2003
Published: December 18, 2003

References

Amir, R.E., Iwai, K., and Ciechanover, A. (2002). The NEDD8 pathway is essential for SCF(β-TrCP)-mediated ubiquitination and processing of the NF-kappa B precursor p105. J. Biol. Chem. *277*, 23253–23259.

Bayer, P., Arndt, A., Metzger, S., Mahajan, R., Melchior, F., Jaenicke, R., and Becker, J. (1998). Structure determination of the small ubiquitin-related modifier SUMO-1. J. Mol. Biol. *280*, 275–286.

Beal, R., Deveraux, Q., Xia, G., Rechsteiner, M., and Pickart, C. (1996). Surface hydrophobic residues of multiubiquitin chains es-

sential for proteolytic targeting. Proc. Natl. Acad. Sci. USA *93*, 861–866.

Bohnsack, R.N., and Haas, A.L. (2003). Conservation in the mechanism of Nedd8 activation by the human AppBp1-Uba3 heterodimer. J. Biol. Chem. *278*, 26823–26830.

Brünger, A.T., Adams, P.D., Clore, G.M., DeLano, W.L., Gros, P., Grosse-Kunstleve, R.W., Jiang, J.S., Kuszewski, J., Nilges, M., Pannu, N.S., et al. (1998). Crystallography & NMR system: a new software suite for macromolecular structure determination. Acta Crystallogr. D Biol. Crystallogr. *54*, 905–921.

Burch, T.J., and Haas, A.L. (1994). Site-directed mutagenesis of ubiquitin. Differential roles for arginine in the interaction with ubiquitin-activating enzyme. Biochemistry *33*, 7300–7308.

Chen, L., Shinde, U., Ortolan, T.G., and Madura, K. (2001). Ubiquitin-associated (UBA) domains in Rad23 bind ubiquitin and promote inhibition of multi-ubiquitin chain assembly. EMBO Rep., 933–938.

DeLano, W.L. (2002). The PyMol User's Manual (San Carlos, CA: DeLano Scientific).

Deng, L., Wang, C., Spencer, E., Yang, L., Braun, A., You, J., Slaughter, C., Pickart, C., and Chen, Z.J. (2000). Activation of the IkappaB kinase complex by TRAF6 requires a dimeric ubiquitin-conjugating enzyme complex and a unique polyubiquitin chain. Cell *103*, 351–361.

Dittmar, G.A., Wilkinson, C.R., Jedrzejewski, P.T., and Finley, D. (2002). Role of a ubiquitin-like modification in polarized morphogenesis. Science *295*, 2442–2446.

Finley, D. (2002). Ubiquitin chained and crosslinked. Nat. Cell Biol. *4*, E121–E123.

Finley, D., Ciechanover, A., and Varshavsky, A. (1984). Thermolability of ubiquitin-activating enzyme from the mammalian cell cycle mutant ts85. Cell *37*, 43–55.

Fisher, R.D., Wang, B., Alam, S.L., Higginson, D.S., Robinson, H., Sundquist, W.I., and Hill, C.P. (2003). Structure and ubiquitin binding of the ubiquitin-interacting motif. J. Biol. Chem. *278*, 28976–28984.

Haas, A.L., Warms, J.V., Hershko, A., and Rose, I.A. (1982). Ubiquitin-activating enzyme. Mechanism and role in protein-ubiquitin conjugation. J. Biol. Chem. *257*, 2543–2548.

Hatfield, P.M., Callis, J., and Vierstra, R.D. (1990). Cloning of ubiquitin activating enzyme from wheat and expression of a functional protein in Escherichia coli. J. Biol. Chem. *265*, 15813–15817.

Hay, R.T. (2001). Protein modification by SUMO. Trends Biochem. Sci. *26*, 332–333.

Hicke, L. (2001). Protein regulation by monoubiquitin. Nat. Rev. Mol. Cell Biol. *2*, 195–201.

Hochstrasser, M. (2000). Evolution and function of ubiquitin-like protein-conjugation systems. Nat. Cell Biol. *2*, E153–E157.

Hoege, C., Pfander, B., Moldovan, G.L., Pyrowolakis, G., and Jentsch, S. (2002). RAD6-dependent DNA repair is linked to modification of PCNA by ubiquitin and SUMO. Nature *419*, 135–141.

Johnson, E.S., Schwienhorst, I., Dohmen, R.J., and Blobel, G. (1997). The ubiquitin-like protein Smt3p is activated for conjugation to other proteins by an Aos1p/Uba2p heterodimer. EMBO J. *16*, 5509–5519.

Kang, R.S., Daniels, C.M., Francis, S.A., Shih, S.C., Salerno, W.J., Hicke, L., and Radhakrishnan, I. (2003). Solution structure of a CUE-ubiquitin complex reveals a conserved mode of ubiquitin binding. Cell *113*, 621–630.

Kurz, T., Pintard, L., Willis, J.H., Hamill, D.R., Gonczy, P., Peter, M., and Bowerman, B. (2002). Cytoskeletal regulation by the Nedd8 ubiquitin-like protein modification pathway. Science *295*, 1294–1298.

Lake, M.W., Wuebbens, M.M., Rajagopalan, K.V., and Schindelin, H. (2001). Mechanism of ubiquitin activation revealed by the structure of a bacterial MoeB-MoaD complex. Nature *414*, 325–329.

Lam, Y.A., Lawson, T.G., Velayutham, M., Zweier, J.L., and Pickart, C.M. (2002). A proteasomal ATPase subunit recognizes the polyubiquitin degradation signal. Nature *416*, 763–767.

Lammer, D., Mathias, N., Laplaza, J.M., Jiang, W., Liu, Y., Callis, J., Goebl, M., and Estelle, M. (1998). Modification of yeast Cdc53p by the ubiquitin-related protein rub1p affects function of the SCFCdc4 complex. Genes Dev. *12*, 914–926.

Liakopoulos, D., Doenges, G., Matuschewski, K., and Jentsch, S. (1998). A novel protein modification pathway related to the ubiquitin system. EMBO J. *17*, 2208–2214.

Liu, J., Furukawa, M., Matsumoto, T., and Xiong, Y. (2002). NEDD8 modification of CUL1 dissociates p120(CAND1), an inhibitor of CUL1–SKP1 binding and SCF ligases. Mol. Cell *10*, 1511–1518.

Loeb, K.R., and Haas, A.L. (1992). The interferon-inducible 15-kDa ubiquitin homolog conjugates to intracellular proteins. J. Biol. Chem. *267*, 7806–7813.

McGrath, J.P., Jentsch, S., and Varshavsky, A. (1991). UBA 1: an essential yeast gene encoding ubiquitin-activating enzyme. EMBO J. *10*, 227–236.

Melchior, F. (2000). SUMO–nonclassical ubiquitin. Annu. Rev. Cell Dev. Biol. *16*, 591–626.

Mizushima, N., Noda, T., Yoshimori, T., Tanaka, Y., Ishii, T., George, M.D., Klionsky, D.J., Ohsumi, M., and Ohsumi, Y. (1998). A protein conjugation system essential for autophagy. Nature *395*, 395–398.

Muller, S., Hoege, C., Pyrowolakis, G., and Jentsch, S. (2001). SUMO, ubiquitin's mysterious cousin. Nat. Rev. Mol. Cell Biol. *2*, 202–210.

Navaza, J. (1994). AMoRe: an automated package for molecular replacement. Acta Crystallogr. A *50*, 157–163.

Ohsumi, Y. (2001). Molecular dissection of autophagy: two ubiquitin-like systems. Nat. Rev. Mol. Cell Biol. *2*, 211–216.

Osaka, F., Kawasaki, H., Aida, N., Saeki, M., Chiba, T., Kawashima, S., Tanaka, K., and Kato, S. (1998). A new NEDD8-ligating system for cullin-4A. Genes Dev. *12*, 2263–2268.

Osaka, F., Saeki, M., Katayama, S., Aida, N., Toh, E.A., Kominami, K., Toda, T., Suzuki, T., Chiba, T., Tanaka, K., et al. (2000). Covalent modifier NEDD8 is essential for SCF ubiquitin-ligase in fission yeast. EMBO J. *19*, 3475–3484.

Otwinowski, Z., and Minor, W. (1997). Processing of X-ray diffraction data collected in oscillation mode. Methods Enzymol. *176*, 307–326.

Pickart, C.M. (2001). Mechanisms underlying ubiquitination. Annu. Rev. Biochem. *70*, 503–533.

Pickart, C.M., Kasperek, E.M., Beal, R., and Kim, A. (1994). Substrate properties of site-specific mutant ubiquitin protein (G76A) reveal unexpected mechanistic features of ubiquitin-activating enzyme (E1). J. Biol. Chem. *269*, 7115–7123.

Polo, S., Sigismund, S., Faretta, M., Guidi, M., Capua, M.R., Bossi, G., Chen, H., P., De Camilli, P., and Di Fiore, P.P. (2002). A single motif responsible for ubiquitin recognition and monoubiquitination in endocytic proteins. Nature *416*, 451–455.

Pozo, J.C., Timpte, C., Tan, S., Callis, J., and Estelle, M. (1998). The ubiquitin-related protein RUB1 and auxin response in Arabidopsis. Science *280*, 1760–1763.

Prag, G., Misra, S., Jones, E.A., Ghirlando, R., Davies, B.A., Horazdovsky, B.F., and Hurley, J.H. (2003). Mechanism of ubiquitin recognition by the CUE domain of Vps9p. Cell *113*, 609–620.

Read, M.A., Brownell, J.E., Gladysheva, T.B., Hottelet, M., Parent, L.A., Coggins, M.B., Pierce, J.W., Podust, V.N., Luo, R.S., Chau, V., et al. (2000). Nedd8 modification of cul-1 activates SCF(β-TrCP)-dependent ubiquitination of IkappaBalpha. Mol. Cell Biol. *20*, 2326–2333.

Rechsteiner, M. (1998). The 26S proteasome. In Ubiquitin and the Biology of the Cell, J.-M. Peters, J.R. Harris, and D. Finley, eds. (New York: Plenum Press), pp. 147–189.

Schwartz, D.C., and Hochstrasser, M. (2003). A superfamily of protein tags: ubiquitin, SUMO and related modifiers. Trends Biochem. Sci. *28*, 321–328.

Shih, S.C., Katzmann, D.J., Schnell, J.D., Sutanto, M., Emr, S.D., and Hicke, L. (2002). Epsins and Vps27p/Hrs contain ubiquitin-binding domains that function in receptor endocytosis. Nat. Cell Biol. *4*, 389–393.

Shih, S.C., Prag, G., Francis, S.A., Sutanto, M.A., Hurley, J.H., and Hicke, L. (2003). A ubiquitin-binding motif required for intramolecular monoubiquitylation, the CUE domain. EMBO J. *22*, 1273–1281.

Sloper-Mould, K.E., Jemc, J.C., Pickart, C.M., and Hicke, L. (2001). Distinct functional surface regions on ubiquitin. J. Biol. Chem. *276*, 30483–30489.

Tateishi, K., Omata, M., Tanaka, K., and Chiba, T. (2001). The NEDD8 system is essential for cell cycle progression and morphogenetic pathway in mice. J. Cell Biol. *155*, 571–579.

VanDemark, A.P., and Hill, C.P. (2003). Two-stepping with E1. Nat. Struct. Biol. *10*, 244–246.

Vijay-Kumar, S., Bugg, C.E., Wilkinson, K.D., and Cook, W.J. (1985). Three-dimensional structure of ubiquitin at 2.8 Å resolution. Proc. Natl. Acad. Sci. USA *82*, 3582–3585.

Walden, H., Podgorski, M.S., and Schulman, B.A. (2003). Insights into the ubiquitin transfer cascade from the structure of the E1 for NEDD8. Nature *422*, 330–334.

Walker, J.E., Saraste, M., Runswick, M.J., and Gay, N.J. (1982). Distantly related sequences in the alpha and beta-subunits of ATP synthase, myosin, kinases and other ATP-requiring enzymes and a common nucleotide binding fold. EMBO J. *1*, 945–951.

Wang, C., Xi, J., Begley, T.P., and Nicholson, L.K. (2001). Solution structure of ThiS and implications for the evolutionary roots of ubiquitin. Nat. Struct. Biol. *8*, 47–51.

Whitby, F.G., Xia, G., Pickart, C.M., and Hill, C.P. (1998). Crystal structure of the human ubiquitin-like protein NEDD8 and interactions with ubiquitin pathway enzymes. J. Biol. Chem. *273*, 34983–34991.

Wilkinson, C.R., Seeger, M., Hartmann-Petersen, R., Stone, M., Wallace, M., Semple, C., and Gordon, C. (2001). Proteins containing the UBA domain are able to bind to multi-ubiquitin chains. Nat. Cell. Biol. *3*, 939–943.

Zheng, J., Yang, X., Harrell, J.M., Ryzhikov, S., Shim, E.H., Lykke-Andersen, K., Wei, N., Sun, H., Kobayashi, R., and Zhang, H. (2002). CAND1 binds to unneddylated CUL1 and regulates the formation of SCF ubiquitin E3 ligase complex. Mol. Cell *10*, 1519–1526.

Accession Numbers

Coordinates for the APPBP1-UBA3-NEDD8 and APPBP1-UBA3-NEDD8-ATP structures have been deposited in the RCSB Protein Data Bank under codes 1R4M and 1R4N.